SL14

# X-RAY DIFFRACTION DETERMINATION OF PEARLITIC STEEL PROPERTIES

**D. Šimek[1], D. Rafaja[1], M. Motylenko[1], V. Klemm[1], G. Schreiber[1],**
**G. Lehmann[2], R. Schmidtchen[2], A. Oswald[2]**

[1]*TU-Bergakademie Freiberg, Materials Science Institute, Gustav Zeuner Str. 5, D-09599 Freiberg*
[2]*TU-Bergakademie Freiberg, Metal Forming Institute, Bernhard von Cotta Str. 4, D-09599 Freiberg*
*simek@fzu.cz*

## Introduction

Ferrito-pearlitic steels are ones of the mostly produced materials for common industrial and construction purposes. The properties of the steel do not depend only on its chemical composition, but on the preparation, i.e. the *thermo-mechanical* history, leading to a different microstructure. The steel is easily-formable at higher temperatures (above 911 °C), when the structure of the steel is fcc cubic (austenite), the recrystallization and recovery takes place and the deformability is practically unlimited. At lower temperatures, primary ferrite (bcc cubic) phase starts to nucleate at grain boundaries, expelling the excessive carbon into the austenite. The amount of primary ferrite depends on the amount of carbon, on the time for which the material is held above the eutectoid temperature (727 °C) and on the grain boundary surface too (cross-section for the diffusion process). The rest austenite decomposes below eutectoid temperature into a mixture of two stable phases – ferrite and cementite (orthorhombic $Fe_3C$). The transformation is of displacive nature (martensitic) but employing a diffusion of excessive carbon away from the newly self-forming ferrite phase. Depending on the undercooling, the transformation occurs during a limited time span, which limits an effective distance the diffusion can affect. The resulting microstructure thus differs from dendritic structure or needle-shaped bainite (for faster cooling) to a lamellar structure called pearlite (slower cooling). The thickness of the lamellas is inversely proportional to the undercooling [1].

### Mechanical properties

The mechanical properties of the resulting pearlite can be roughly described as follows: The yield stress of pearlite is inversely proportional to a certain power of its interlamellar spacing $S$:

$$_{y/u} \quad _0 \quad K \; S^{m_h} \qquad (1)$$

The equation is referred to as Hall-Petch relationship and originally describes an enhancement of the yield stress with the refinement of the grains ($m_h = 1/2$). The extrapolation to an infinitely thick lamellas $_0$ yields negative values for $m_h = 1/2$, thus $m_h = 1$ is usually considered. Alternatively an expression based on the dislocation motion in within lamellas was derived [2], where $\sim S^{-1}\ln(SV \; b)$, $b$ is the Burgers vector and $V$ a volume portion of ferrite in pearlite. This expression is equivalent to (1) and $m_h = 1$ for large $S$ and deviates towards $m_h = 1/2$ for thinner lamellas. The past studies of fully pearlitic eutectoid and hypereutectoid (carbon content 0.73 wt.%) steels [3, 4]

with experimental values of $S$ typically ranging from 150 to 250 nm did not allow to determine properly the nature of the dependence.

The behaviour of the hypoeutectoid (carbon content < 0.73 wt.%) steel is even more complex, as it is a composite formed from primarily crystallized ferrite grains with a size at the order of microns and the pearlitic colonies of similar size (several microns). The combination of micro- and nano-scale originated effects superimpose and the early investigations of yield stress [3] were not much successful in description of the composite behaviour. Recently, self-consistent simulation procedures were introduced [5], which allow modeling of the stress-strain curves at higher stages of deformation at least.

## Experimental

The samples were hot-rolled under different temperatures in an industrial type of rolling stage with one to 14 passes through the rolls. After the rolling, the resulting circular or elliptical profile was cooled down either on the air, in the water, in a molten lead bath or their combination (e.g. first rest on the air, then lead bath). The aim was to produce a variety of microstructures with different mechanical properties. Specimen of the resulting materials were cut (both normally and laterally), embedded into a resin matrix, ground, polished and etched. The resulting surface (originally inside the profile) was investigated by means X-ray diffraction on a Bragg-Brentano goniometer and also metallographically investigated in an optical microscopy and scanning electron microscopy (SEM). SEM allowed to determine basic microstructural parameters (volume portion of pearlite and mean pearlite interlamellar spacing) directly. The choice of samples for detailed metallographic investigation was made upon the results obtained from X-ray diffraction.

### X-Ray diffraction results

The diffraction revealed a presence of residual stress in the steel, which is expressed as an anisotropic shift of the diffraction lines [6]. The reason could be the partial coherence of certain crystallographic planes of ferrite and cementite in the pearlite arising from the displacive nature of the eutectoid transformation. Furher on, an anisotropic dislocation-originated broadening was observed (Fig. 1). The magnitude and anisotropy of the integral breadth was evaluated according to

$$_{hkl}^2 \quad _{inst}^2 (\;_{hkl}) \quad _{size}^2 \quad _{disl}^2 (1 \; q)\;_{hkl} \frac{16}{2}\sin^2 \;_{hkl} \qquad (2)$$
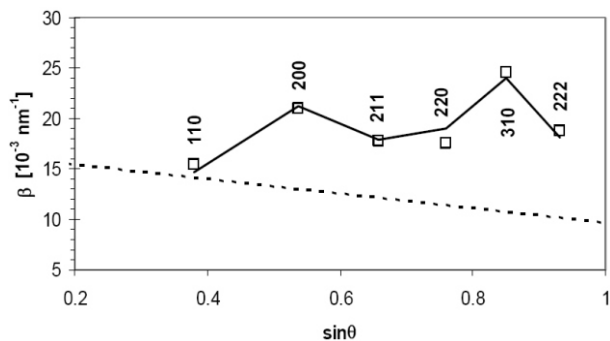
**Figure 1.** Typical Williamson-Hall plot of the ferrite diffraction lines broadening. Broken line corresponds to instrumental broadening, cranky line connects the fitted theoretical values.
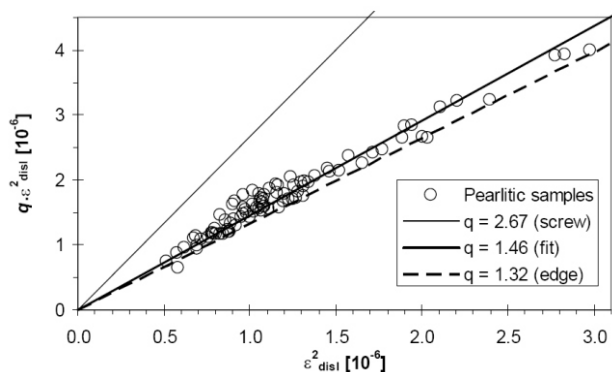


**Figure 2.** Squared dislocation microstrain and its anisotropy observed in diffraction line broadening.
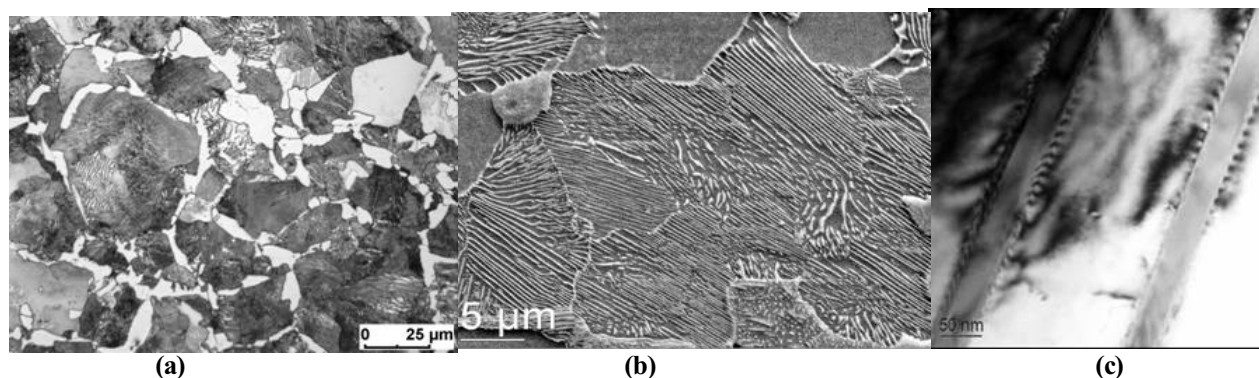


**Figure 3.** Optical microscopy (a) and scanning electron microscopy (b) image of ferrito-pearlitic steel and a detailed transmission electron microscopy (c) image of ferrite and cementite lamellas in the pearlite.

Here    is the radiation wavelength, $_{inst}$ instrumental broadening, $_{size}$ broadening due to a finite coherent domain size (negligible) and $_{disl}$ a root-mean-square microstrain in $100$ direction, the anisotropy the microstrain is described by parameter $q$ [7]. The resulting values of $q \times \, ^2_{disl}$ are plotted versus $^2_{disl}$ in Figure 2, the $q$ parameter corresponds well with the expected presence of edge dislocations with Burgers vector $\boldsymbol{b} = a/2 \times \, 111$. The magnitude of squared dislocation microstrain differs by almost one order for different pearlitic samples, so differs also the density of the dislocations.

### Microscopy

Figure 3 shows a microscopic view on the ferrito-pearlitic steel in three different magnifications. Optical microscopy (Fig. 3a) can be exploited to determine the pearlite volume fraction, since primary ferrite is displayed as light areas. SEM allows to gain a mean interlamellar spacing in pearlite by means of statistical methods [8]. The transmission electron microscopy (TEM) was utilised to reveal the details of microstructure. As obvious in Figure 3c, there are deformation fields present on the ferrite-cementite interface in pearlite. The origin of these can be found in the presence of misfit dislocations accommodating the difference in lattice spacing of the originally continuous lattice planes (before the transformation). The dislocations are almost equally spaced in a particular pearlitic colony and their mutual dis-

tance ranges from 20 to 30 nanometres. The primary ferrite grains as well as the inner volume of the ferritic lamellas in pearlite are practically free of any dislocation.

### Results

The assumption was made that the misfit dislocations are responsible for the X-ray diffraction line broadening. Another assumption was made that the density of the dislocations is proportional to the density of the lamellas. Together, the dislocation squared magnitude of the dislocation line broadening (or the squared dislocation originated
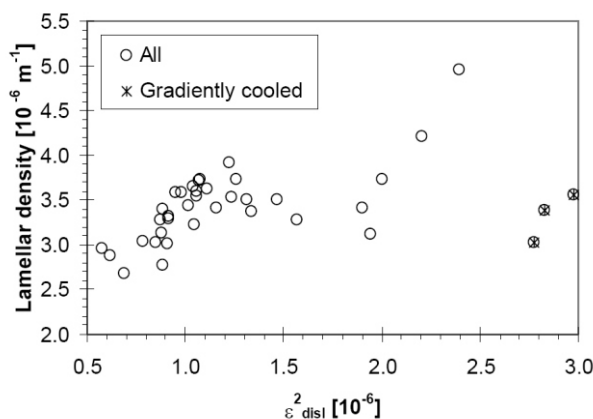


**Figure 4.** Correlation of lamellar density and dislocation originated squared microstrain

microstrain) should be proportional to the density of the lamellas (Fig. 4). Ultimate tensile stress (UTS) is roughly proportional to the weighted average of the pearlite and ferrite strength. The strength of the pearlite is inversely proportional to its interlamellar spacing (1), thus even UTS should be proportional to the density of lamellas, moreover to the squared dislocation microstrain (Fig. 5).

## References

1. R. F. Mehl, W. C. Hagel, *Progress in Metal Physics* **6**, (1956), pp. 74-134.

2. L. M. Brown & R. K. Ham, in *Strengthening Methods in Crystals*, edited by A. Kelly & R. B. Necholson, London, 1971, p. 12.

3. K. K. Ray, D. Mondal, *Acta Metall. Mater.* **39**, (1991), pp. 2201-2208.

4. A. M. Elwazri, P. Wanjara, S. Yue, *Mat. Sci. Eng. A* **404**, (2005), pp. 91-98.

5. S. Allain, O. Bouaziz, *Mat. Sci. Eng. A* **496**, (2008), pp. 329-336.

6. D. Šimek, D. Rafaja, M. Motylenko, V. Klemm, G. Schreiber, A. Brethfeld, G. Lehmann, *Steel Research Int.* **79**, (2008), pp. 800-806.

7. T. Ungár, I. Dragomir, Á. Révész, A. Borbély, *J. Appl. Cryst.* **32**, (1999), pp. 992-1002.
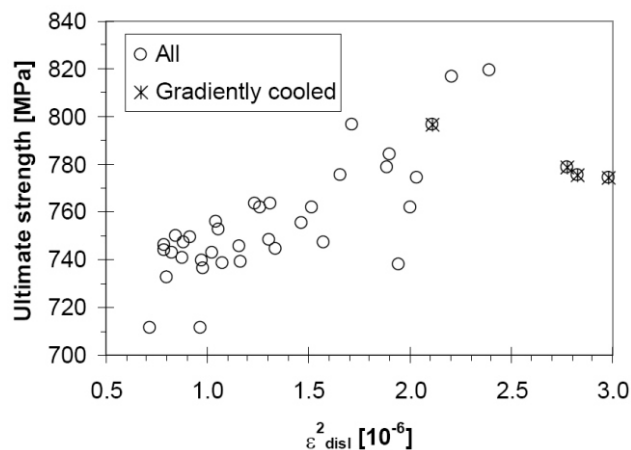
**Figure 5.** Correlation of ultimate tensile stress and dislocation originated squared microstrain.

8. J. Ohser & U. Lorz, in *Freiberger Forschungshefte B* **276**, Technischer Verlag für Grundstoffindustrie, Leipzig, Stuttgart, 1994, p. 104.

## Acknowledgements

---

**SL15**

### SiGe products prepared by CVD from different precursors

## SiGe PRODUKTY PŘIPRAVENÉ METODOU CVD Z RŮZNÝCH PREKURZORŮ

### M. Klementová[1,3], V. Dřínek[2], L. Palatinus[1], M. Rieder[4]

[1]*Fyzikální ústav AV ČR, v.v.i., Cukrovarnická 10, 162 00 Praha, Česká republika*
[2]*Ústav chemických procesů AV ČR, v.v.i., Rozvojová 135, 165 02 Praha*
[3]*Ústav anorganické chemie AV ČR, v.v.i., 250 68 Husinec-Řež, Česká republika*
[4]*Česká geologická služba, Geologická 6, 150 00 Praha 5, Česká republika*
*klemari@fzu.cz*

### Úvod

Nanomateriály jsou v současné době středem zájmu pro svoje specifické chemické a fyzikální vlastnosti, které se díky jejich velikosti liší od vlastností ekvivalentních fází ve velkém objemu. V mikroelektronice jsou velice žádané nanoobjekty vyrobené z polovodičů, křemíku a germania, případně jejich kombinací ve např. ve formě strukturovaných nanovláken či slitiny SiGe. Přítomnost germania umožňuje rychlejší přenos informace v integrovaných obvodech vzhledem k jeho vyšší elekronové mobilitě ve srovnání s křemíkem (Ge - 3900 cm$^2$/V.s; Si - 1500 cm$^2$/V.s).

Metoda CVD (Chemical Vapour Deposition) je běžná technika pro přípravu nanoobjektů (nanovláken, nanotrubiček, nanodestiček atd.). Využívá prekurzory, jejichž páry jsou vedeny do vyhřívaného reaktoru, kde jsou pyrolyticky dekomponovány za vzniku pevných produktů.

### Metody

Vzorky byly připraveny pyrolýzou prekurzorů za použití techniky LPCVD (Low Pressure Chemical Vapour Deposition). Byly použity dva rozdílné prekurzory a jim odpovídající nastavení aparatury. Vzorky připravené pyrolýzou tris(trimethylsilyl)germanu $(Si(CH_3)_3)_3GeH$ byly deponovány na tantalovou podložku při teplotě 365 °C po dobu 90 minut. Pyrolitická aparatura pracovala v průtočném módu při tlaku 90 – 100 Pa. Vzorky připravené pyrolýzou hexamethyldigermanu $Ge_2(CH_3)_6$ společně s ethylsilanem $(C_2H_5)SiH_3$ byly deponovány na měděnou podložku při teplotě 500 °C po dobu 70 minut. Pyrolitická aparatura pracovala v průtočném módu při celkovém tlaku 180 Pa, z čehož bylo 110 Pa $Ge_2(CH_3)_6$ a 70 Pa $(C_2H_5)SiH_3$.

Vzorky byly studovány elektronovou mikroskopií (SEM, TEM, HRTEM) a elektronovou difrakcí (SAED, PED).